

# A k-distribution technique for radiative transfer simulation in inhomogeneous atmosphere:

## 2. FKDM, fast k-distribution model for the shortwave

Boris Fomin and Marcelo de Paula Correa

Centro de Previsão de Tempo e Estudos Climáticos, Instituto Nacional de Pesquisas Espaciais, Cachoeira Paulista, São Paulo, Brazil

Received 25 June 2004; revised 15 October 2004; accepted 12 November 2004; published 19 January 2005.

[1] A new technique for developing k-distributions applied to longwave radiation parameterization has been presented in a preceding paper. Now we discuss an extension of this technique to the shortwave spectral range. A fast k-distribution model (FKDM) for gaseous absorption calculations suitable for use in weather and climate prediction is described. FKDM has been created using 15 k-distribution terms only, less than in other comparable codes. The molecular species represented in the model are H<sub>2</sub>O, CO<sub>2</sub>, O<sub>3</sub>, and O<sub>2</sub>. In k-distribution terms, characterized by strong absorption, representative absorption cross section is treated as a function of absorber amount along the direct solar radiation path, thus allowing improved fitting of solar fluxes and heating rates in upper troposphere and stratosphere. This technique has been applied to derive effective single-scattering properties of clouds in each term for a more accurate treatment of cloud optical properties by taking into account correlation between water vapor and liquid water or ice absorption. It is shown that disregarding the above correlation in radiation models can essentially distort simulated fluxes and heating rates. FKDM has been developed and validated using a fast line-by-line model (FLBLM). Both FKDM and FLBLM used a Monte-Carlo code. Validations have covered the tropical, midlatitude summer, midlatitude winter, subarctic summer, subarctic winter, and U.S. standard atmospheres, four atmospheres from the Spectral Radiance Experiment campaign, and a case of an observed tropical atmosphere. It is found that the FKDM heating rate accuracy for clear-sky conditions is as follows:  $\sim 0.1$  and  $\sim 0.2$  K d<sup>-1</sup> in the troposphere for standard and real atmospheres, respectively, and  $\sim 0.5$  K d<sup>-1</sup> in all the cases at altitudes below 70 km. Downward flux errors are below 1%, upward flux errors are below 2% (usually  $\sim 1.5$  W m<sup>-2</sup>), and total atmospheric absorption errors are below 3% (usually 1.5–3 W m<sup>-2</sup>) in every case. The Intercomparison of Radiation Codes in Climate Models (ICRCCM) cloud models have also been used for the validations. It has been demonstrated that the usage of the technique to derive effective cloud optical properties halves maximal errors in calculated radiation fluxes absorbed by cloud.

**Citation:** Fomin, B., and M. de P. Correa (2005), A k-distribution technique for radiative transfer simulation in inhomogeneous atmosphere: 2. FKDM, fast k-distribution model for the shortwave, *J. Geophys. Res.*, 110, D02106, doi:10.1029/2004JD005163.

### 1. Introduction

[2] A new effective k-distribution technique and its application for the longwave radiation parameterization have recently been discussed in a preceding paper [Fomin, 2004] (hereinafter referred to as part 1). Since both the technique and its comparison with other k-distribution methods are thoroughly discussed in part 1, in the present paper (part 2) we will discuss only its extension to the shortwave spectral region. Here it is necessary to consider

shortwave fluxes and heating rates instead of longwave fluxes and cooling rates. It should be noted that shortwave downward flux is usually much greater than the upward flux in contrast to situation in the longwave radiation (due to molecular and cloud/aerosol absorption of solar radiation within atmosphere and absorption by surface). For this reason, in the present work, we only used line-by-line (LBL) downward fluxes for k-distribution development.

[3] Since this technique gives a possibility to obtain the shortest k-distribution series achievable in practice and the computational time is proportional to the number of terms in the k-distribution series, our objective was to develop the

**Table 1.** Formulae for Volume Absorption Coefficients<sup>a</sup>

| Channel | Formula   |
|---------|---|
| 1       | $\bar{K}(O_3) * U_{O_3} + \bar{K}(O_2) * U_{O_2}$   |
| 2       | $\bar{K}(O_3) * U_{O_3}$  |
| 3       | $1.93 \cdot 10^{-21} * U_{O_3} + 2 \cdot 10^{-26} * U_{H_2O}$   |
| 4       | $\bar{K}(O_2) * U_{O_2}$  |
| 5       | $\{1.35 \times 10^{-25} * [1 - 0.0007 * (300 - T)] * P^{0.77}\} * U_{H_2O} + 1.19 \times 10^{-27} * P^{0.59} * U_{O_2} + 1.7 \times 10^{-22} * U_{O_3}$                         |
| 6       | $2.1 \times 10^{-24} * P^{0.55} * U_{H_2O} + 1.4 \times 10^{-22} * U_{O_3}$   |
| 7       | $\bar{K}(H_2O) * U_{H_2O}$  |
| 8       | $\bar{K}(CO_2) * U_{CO_2} + \bar{K}(H_2O) * U_{H_2O}$   |
| 9       | $\{3.77 \times 10^{-25} * [1 - 0.00372 * (300 - T)] * P^{0.65}\} * U_{H_2O} + 6.5 \times 10^{-49} * 3.2^{(300-T)/43} * U_{H_2O}^2 + 1.55 \times 10^{-24} * P^{0.54} * U_{CO_2}$ |
| 10      | $\bar{K}(H_2O) * (300/T_S)^{1.3} * U_{H_2O} + 6.5 \times 10^{-48} * 3.2^{(300-T)/43} * U_{H_2O}^2 + 2.09 \times 10^{-24} * P^{0.626} * U_{CO_2}$                                |
| 11      | $\bar{K}(H_2O) * (300/T_S)^{2.1} * U_{H_2O} + 2.5 \times 10^{-47} * 3.2^{(300-T)/43} * U_{H_2O}^2 + 2.60 \times 10^{-24} * P^{0.606} * U_{CO_2}$                                |
| 12      | $\bar{K}(H_2O) * (300/T_S)^{1.2} * U_{H_2O} + 8.0 \times 10^{-47} * 3.2^{(300-T)/43} * U_{H_2O}^2 + 6.85 \times 10^{-25} * P^{0.518} * U_{CO_2}$                                |
| 13      | $\{1.3 \times 10^{-24} * [1 - 0.00235 * (300 - T)] * P^{0.65}\} * U_{H_2O} + 6.0 \times 10^{-48} * 3.2^{(300-T)/43} * U_{H_2O}^2 + 1.99 \times 10^{-24} * P^{0.782} * U_{CO_2}$ |
| 14      | $\bar{K}(H_2O) * U_{H_2O} + 2.6 \times 10^{-47} * 3.2^{(300-T)/43} * U_{H_2O}^2 + 9.49 \times 10^{-25} * P^{0.609} * U_{CO_2}$  |
| 15      | $\bar{K}(H_2O) * U_{H_2O} + 2.0 \times 10^{-46} * 3.2^{(300-T)/25} * U_{H_2O}^2 + 3.64 \times 10^{-24} * P^{0.799} * U_{CO_2}$  |

<sup>a</sup>Volume absorption coefficients are in  $\text{km}^{-1}$ . P and T are pressure and temperature (in atm and K). The notations  $\bar{K}(O_3)$ ,  $\bar{K}(O_2)$ ,  $\bar{K}(H_2O)$ , and  $\bar{K}(CO_2)$  mean the representative cross sections as functions of species amounts along the direct solar radiation from TOA to the given point, which can be calculated using Table 2. The notations  $U_{O_3}$ ,  $U_{O_2}$ ,  $U_{H_2O}$ , and  $U_{CO_2}$  mean  $O_3$ ,  $O_2$ ,  $H_2O$ , and  $CO_2$  concentrations (in molecules/ $\text{cm}^2$  km), respectively, at the given point.

fastest k-distribution parameterization, suitable for use in weather and climate prediction. The fast k-distribution model (FKDM) for gas absorption calculations is presented. The corresponding model for simulation of solar radiation in clear-sky, hazy and cloudy plane-parallel atmospheres has been developed, where we treat molecular and particulate scattering by means of Monte-Carlo method [Fomin and Mazin, 1998].

[4] In this FKDM version we considered absorption by  $H_2O$ ,  $CO_2$ ,  $O_3$  and  $O_2$  that needs only 15 k-distribution terms (channels). In the channels where absorption is strong, representative absorption cross section is treated as

a function of absorber amount along the direct solar radiation path. This unique feature is responsible for the improved fitting of solar fluxes and heating rates in upper troposphere and stratosphere.

[5] Fast radiation parameterizations usually use a few broad spectral bands with effective scattering and absorption coefficients of clouds and aerosols in each band. Here we use the same set of three IR spectral bands for k-distributions that is used in the widely distributed parameterization by Chou and Suarez [2002] to facilitate the use of their optical cloud and aerosol models. In addition, we also use effective scattering and absorption

**Table 2.** Points of Interpolation for Representative Cross Sections K as a Function of the Species Amount W<sup>a</sup>

| Channel | Species | Values     | Point of Interpolation |       |       |        |       |       |       |       |       |       |       |         |      |       |      |  |  |
|---------|---------|------------|------------------------|-------|-------|--------|-------|-------|-------|-------|-------|-------|-------|---------|------|-------|------|--|--|
|         |         |            | 1                      | 2     | 3     | 4      | 5     | 6     | 7     | 8     | 9     | 10    | 11    | 12      | 13   | 14    | 15   |  |  |
| 1       | $O_3$   | W (*1E17)  | 1E-6                   | 0.02  | 0.05  | 0.1    | 0.2   | 0.4   | 0.6   | 1.0   | 2.0   | 3.0   | 4.0   |         |      |       |      |  |  |
| 1       | $O_3$   | K (*1E-18) | 3.65                   | 3.65  | 3.62  | 3.55   | 3.45  | 3.2   | 3.0   | 2.6   | 1.85  | 1.5   | 1.2   |         |      |       |      |  |  |
| 1       | $O_3$   | W (*1E17)  | 5.0                    | 6.0   | 7.0   | 9.0    | 15.0  | 20.0  | 30.0  | 100.0 | 200.0 | 250.0 | 400.0 |         |      |       |      |  |  |
| 1       | $O_3$   | K (*1E-18) | 1.05                   | 0.95  | 0.9   | 0.8    | 0.63  | 0.57  | 0.47  | 0.32  | 0.26  | 0.23  | 0.05  |         |      |       |      |  |  |
| 1       | $O_2$   | W (*1E22)  | 1E-07                  | 0.1   | 1.0   | 4.0    | 10.0  | 70.0  | 200.0 |       |       |       |       |         |      |       |      |  |  |
| 1       | $O_2$   | K (*1E-25) | 3.4                    | 3.4   | 3.3   | 3.05   | 2.4   | 0.6   | 0.25  |       |       |       |       |         |      |       |      |  |  |
| 2       | $O_3$   | W (*1E17)  | 1E-6                   | 7E-4  | 0.4   | 2.0    | 7.0   | 20.0  | 50.0  | 100.0 |       |       |       |         |      |       |      |  |  |
| 2       | $O_3$   | K (*1E-20) | 7.35                   | 7.35  | 8.35  | 8.0    | 7.5   | 7.0   | 6.0   | 5.5   |       |       |       |         |      |       |      |  |  |
| 4       | $O_2$   | W (*1E22)  | 0.01                   | 0.05  | 0.1   | 0.3    | 1.0   | 3.0   | 10.0  | 100.0 |       |       |       |         |      |       |      |  |  |
| 4       | $O_2$   | K (*1E-24) | 1.9                    | 1.8   | 1.5   | 1.0    | 0.7   | 0.48  | 0.25  | 0.25  |       |       |       |         |      |       |      |  |  |
| 7       | $H_2O$  | W (*1E21)  | 0.001                  | 0.01  | 0.03  | 0.1    | 1.0   | 3.0   | 20.0  | 100.0 | 200.0 |       |       |         |      |       |      |  |  |
| 7       | $H_2O$  | K (*1E-23) | 7.61                   | 6.85  | 6.52  | 5.98   | 3.81  | 2.72  | 1.63  | 1.09  | 0.978 |       |       |         |      |       |      |  |  |
| 8       | $H_2O$  | W (*1E20)  | 1E-5                   | 5E-6  | 1E-4  | 4E-4   | 0.001 | 0.005 | 0.01  | 0.05  | 0.1   | 0.7   | 4.0   | 20.0    | 80.0 | 200.0 | 1E+3 |  |  |
| 8       | $H_2O$  | K (*1E-22) | 40                     | 60    | 70    | 60     | 45    | 20    | 14    | 17.8  | 17.5  | 8.0   | 3.0   | 0.5     | 0.1  | 0.04  | 0.01 |  |  |
| 8       | $CO_2$  | W (*1E19)  | 4E-5                   | 1E-4  | 4E-4  | 0.002  | 0.01  | 0.1   | 1.0   | 10.0  | 100.0 | 1E+3  |       |         |      |       |      |  |  |
| 8       | $CO_2$  | K (*1E-21) | 80                     | 50    | 25    | 10     | 6.0   | 2.0   | 0.8   | 0.45  | 0.25  | 0.13  |       |         |      |       |      |  |  |
| 10      | $H_2O$  | W (*1E22)  | 0.001                  | 0.01  | 0.1   | 0.4    | 1.0   | 4.0   | 7.0   | 10.0  | 20.0  | 100.0 |       |         |      |       |      |  |  |
| 10      | $H_2O$  | K (*1E-24) | 1.8                    | 2.34  | 3.19  | 4.03   | 4.67  | 6.05  | 6.26  | 6.37  | 6.26  | 5.84  |       |         |      |       |      |  |  |
| 11      | $H_2O$  | W (*1E22)  | 0.001                  | 0.01  | 0.1   | 1.0    | 2.0   | 4.0   | 10.0  | 100.0 |       |       |       |         |      |       |      |  |  |
| 11      | $H_2O$  | K (*1E-23) | 0.823                  | 1.65  | 2.35  | 3.29   | 3.53  | 3.47  | 2.7   | 1.76  |       |       |       |         |      |       |      |  |  |
| 12      | $H_2O$  | W (*1E21)  | 1E-4                   | 0.001 | 0.005 | 0.0105 | 0.02  | 0.2   | 0.7   | 2.0   | 5.0   | 20.0  | 100.0 | 1E+3    |      |       |      |  |  |
| 12      | $H_2O$  | K (*1E-22) | 17.0                   | 12.2  | 8.5   | 8.78   | 7.56  | 4.25  | 2.55  | 1.89  | 1.42  | 0.85  | 0.283 | 9.45E-3 |      |       |      |  |  |
| 14      | $H_2O$  | W (*1E22)  | 1E-4                   | 0.001 | 0.01  | 0.1    | 1.0   | 2.0   | 4.0   | 10.0  | 15.0  | 20.0  | 100.0 |         |      |       |      |  |  |
| 14      | $H_2O$  | K (*1E-23) | 0.209                  | 0.313 | 0.584 | 0.834  | 1.3   | 1.46  | 1.49  | 1.25  | 1.1   | 1.04  | 0.834 |         |      |       |      |  |  |
| 15      | $H_2O$  | W (*1E21)  | 1E-5                   | 1E-4  | 0.001 | 0.01   | 0.1   | 1.0   | 3.0   | 10.0  | 40.0  | 100.0 |       |         |      |       |      |  |  |
| 15      | $H_2O$  | K (*1E-22) | 74.9                   | 41.6  | 11.7  | 16.6   | 7.49  | 2.5   | 1.25  | 0.666 | 0.499 | 0.25  |       |         |      |       |      |  |  |

<sup>a</sup>Representative cross sections K are given in  $\text{cm}^2/\text{molecule}$ ; species amounts W are given in  $\text{molecules}/\text{cm}^2$ .

coefficients of clouds in each k-distribution channel (in the same way as for gaseous absorption) for taking into account the correlation between water vapor and liquid water (and ice) absorption. As will be shown, this technique allows a more accurate treatment of cloud optical properties in radiation parameterizations.

[6] For FKDM development and validation a fast line-by-line model (FLBLM) [Fomin, 1994; Fomin and Mazin, 1998] has been used, which rigorously treats radiation scattering and absorption by means of Monte-Carlo method. The latest HITRAN-11v spectral database [Rothman et al., 2003] as well as the recent H<sub>2</sub>O (CKD-2.4 version), O<sub>2</sub> and O<sub>3</sub> continuum models [Mlawer et al., 1999] are used in this FLBLM version in accordance with the recommendation from Fomin et al. [2004]. A solar spectrum was taken from MODTRAN (usually referred to as the Kurucz spectrum (<http://cfaku5.harvard.edu/sun/irradiance/irradiancebins.dat>)). It should be noted that FLBLM has been validated in a recent effort involving intercomparison of shortwave radiation transfer codes and measurements [Halothore et al., 2005] as well as using other efforts involving LBL calculations [Fomin et al., 2004; Ptashnik and Shine, 2003].

[7] In section 2 we present a detailed description of this new technique to generate k-distributions. Section 3 is devoted to the treatment of cloud optical properties in k-distribution models. Finally, in section 4 we provide a summary of the main results. Detailed parameters of FKDM are presented in Tables 1 and 2.

## 2. Molecular Absorption and Scattering

[8] In this version of FKDM we have used three bands in UV and VIS regions (14,280–31,000), (31,000–33,000) and (33,000–50,000) cm<sup>-1</sup> as well as three bands in the IR region (1000–4400), (4400–8200) and (8200–14,280) cm<sup>-1</sup> for reasons that will be explained in section 3. It is possible to consider only one channel (k-distribution term) in each of the UV or VIS band [Chou and Suarez, 2002; Kato et al., 1999; Briegleb, 1992]. In this simplest case our technique reduces to finding the effective absorption coefficients profile  $K(W)$  and then representative cross-section profile  $\bar{K}(W)$  as a function of the absorber amount  $W$  along the direct solar radiation path, which exactly reproduces the LBL downward solar flux in the band considered. Consequently in this case our technique is close to that of Chou and Suarez [2002] (see their formulae (3.7) and (3.13)), with only one difference: they use the mean transmission function of the absorber amount along the vertical whereas we usually considered the downward flux at the solar zenith angle  $SZA = 30^\circ$  for the tropical or subarctic winter atmospheres. Obviously, if absorption is weak (the transmission function is a linear function of  $W$ ), the representative cross sections equal mean values of real cross sections in the given spectral band weighted by the extraterrestrial solar flux (see equation 3.12 of Chou and Suarez [2002]). It is important to note that real cross sections in the UV and VIS spectral regions are practically independent of pressure and temperature because they mainly consist of the electronic bands of O<sub>3</sub> and O<sub>2</sub> [Goody and Yung, 1989; Chou and Suarez, 2002]. Therefore the ozone representative absorption cross section in

the 14,280–31,000 cm<sup>-1</sup> band was taken to have a constant value equal to  $1.93 \times 10^{-21}$  cm<sup>2</sup>/molecule. It should be stressed that absorption in this band is weak (the mean ozone optical thickness is about 0.02). However, in a typical case, the representative cross section  $\bar{K}$  varies with  $W$  from the above mean value (at  $W \rightarrow 0$ ) to the minimum cross section in the given spectral region  $\bar{K}_{\min}$  (at  $W \rightarrow \infty$ ). To explain this statement let us write the LBL and one-term k-distribution formulae for the downward flux  $F_{\downarrow}(W)$  (scattering is omitted here):

$$F_{\downarrow}(W) = (S_1 e^{-K_1 W} + S_2 e^{-K_2 W} + \dots + S_M e^{-K_M W} + \dots + S_N e^{-K_N W}) = S e^{-\tau(W)}, \quad (1)$$

where  $S_1, S_2, \dots, S_N$  and  $K_1, K_2, \dots, K_N$  are the solar irradiance and absorption coefficient considered at  $N$  points of some LBL wave number grid, index  $M$  denotes the wave number point with the weakest absorption,  $S = (S_1 + S_2, \dots, S_N)$  is the solar extraterrestrial flux in the given spectral band and  $\tau(W)$  is the effective optical thickness in our k-distribution approximation. It is clear that at  $W \rightarrow \infty$  the term  $S_M e^{-K_M W}$  will be dominated and we can write

$$\begin{aligned} (\text{at } W \rightarrow \infty) S e^{-\tau(W)} &\approx S_M e^{-K_M W}; \\ \tau(W)/W &= [K_M W + \ln(S/S_M)]/W \rightarrow K_M. \end{aligned} \quad (2)$$

[9] The last expression explains the statement. Figure 1, where the 33,000–50,000 cm<sup>-1</sup> spectral region is considered (the mean optical thickness is about 30), demonstrates the typical behavior of  $\bar{K}(W)$ .

[10] In view of this, more narrow bands are usually used in parameterizations to get approximately constant values of representative cross sections. For example, Chou and Suarez [2002] used four and eight spectral bands in 33,900–57,140 cm<sup>-1</sup> and 14,280–57,140 cm<sup>-1</sup> spectral regions, respectively. In contrast to their and other present parameterizations, we suggest direct usage of  $\bar{K}(W)$  in a case of strong absorption (optical thickness  $\sim 10$ ) in order to use the essentially wider spectral intervals and thus to decrease the number of k-distribution terms. Here we made use of independence of the representative cross sections  $\bar{K}(W)$  on atmospheric conditions and the solar zenith angle (SZA), which is a consequence of independence of the real cross sections on pressure and temperature. Naturally,  $\bar{K}(W)$ , because of their obtaining from the downward fluxes, can exactly fit only the downward fluxes and may not be suitable for fitting upward fluxes or scattered radiation with very high accuracy. However, if absorption is strong enough, solar radiation does not reach the surface and the adjacent scattering atmospheric layers (clouds, aerosols and thick air), so that only direct solar radiation needs to be fitted. In the case of moderate absorption, where solar radiation reaches the surface, it is necessary to use narrower band. So in FKDM we used the 31,000–33,000 cm<sup>-1</sup> band with a mean optical thickness of about 0.7. However, in the case of weak absorption, where the mean cross section is applicable, the band can be wide again for the reason explained above. Therefore we use only three spectral bands (or channels), (4280–31,000), (31,000–33,000) and (33,000–50,000) cm<sup>-1</sup> in VIS + UV with

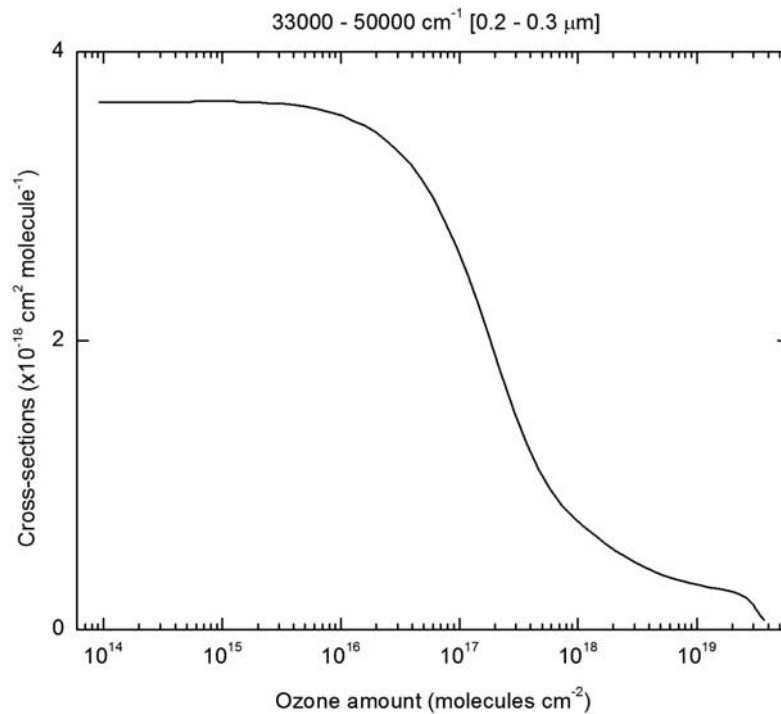


**Figure 1.**  $\text{O}_3$  representative cross section  $\bar{K}(W)$  as a function of ozone amount  $W$  along the direct solar radiation path in the  $33,000\text{--}50,000\text{ cm}^{-1}$  spectral region.

strong, moderate and weak ozone absorption, instead of 8 bands in the work of *Chou and Suarez* [2002], 16 bands in the work of *Kato et al.* [1999], 8 bands in the work of *Briegleb* [1992], 7 channels in the work of *Cusack et al.* [1999], and 7 channels in the work of *Nakajima et al.* [2000]. [11] In addition to ozone absorption in VIS and UV, the absorption by oxygen (the last line in the HITRAN-11v is

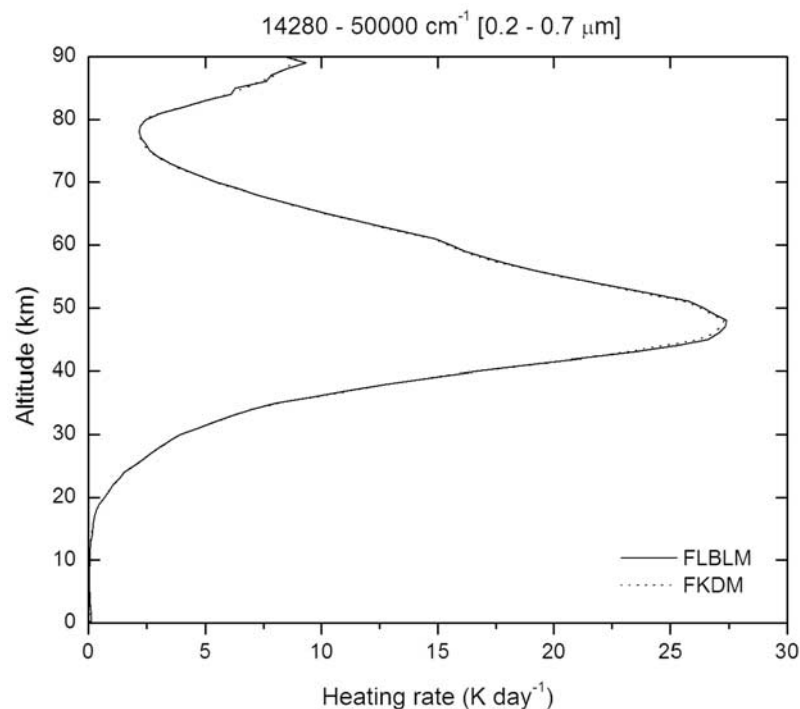


**Figure 2.** Referenced FLBLM (solid line) and approximate FKDM (dotted line) heating rates in the  $14,280\text{--}50,000\text{ cm}^{-1}$  region. Absorption by ozone, oxygen, and water vapor is considered in the MLS atmosphere at  $\text{SZA} = 30^\circ$  and surface albedo = 0.2. Molecular scattering is neglected.

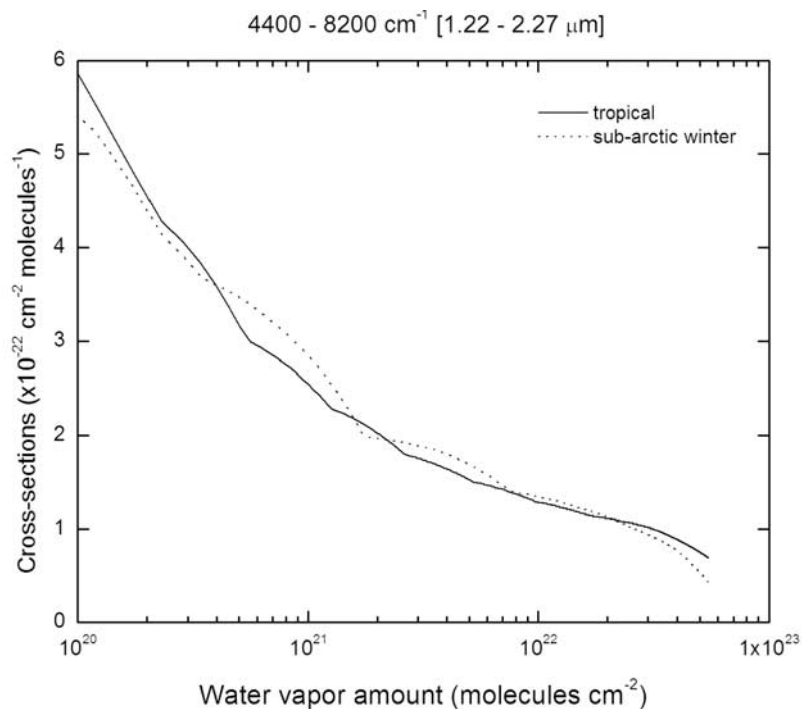


**Figure 3.** H<sub>2</sub>O representative cross sections in the most absorbing channel of the 4400–8200 cm<sup>-1</sup> region obtained for tropical (solid line) and subarctic winter (dotted line) atmospheres at SZA = 30° and SZA = 75°, respectively.

at 15,927 cm<sup>-1</sup>, Herzberg continuum from 36,000 cm<sup>-1</sup>) and relatively weak absorption by water vapor (the last line is at 22,656 cm<sup>-1</sup>) were taken into account in FKDM. The Herzberg continuum was taken into account in the 33,000–50,000 cm<sup>-1</sup> band in the same way that the ozone absorption was (the optical thickness of oxygen is about 2). For the water vapor absorption we also used a constant value of  $2 \times 10^{-26}$  cm<sup>2</sup>/molecule as the representative cross section in the 14,280–31,000 cm<sup>-1</sup> band (the optical thickness of water vapor here is less than  $\sim 0.003$ ). It is important to note that *Chou and Suarez* [2002] also used constant representative cross section for H<sub>2</sub>O in VIS.

[12] This 3-band parameterization is notably accurate. For example in clear-sky conditions it fits the heating rates related to the ozone absorption with accuracy better than  $\sim 0.2$  K d<sup>-1</sup> or  $\sim 1\%$  whereas other parameterizations usually have accuracy about 1 K d<sup>-1</sup> [e.g., *Chou and Lee*, 1996]. Figure 2 illustrates the typical FLBLM and FKDM heating rates in the 14,280–50,000 cm<sup>-1</sup> region. Here absorption by ozone, oxygen and water vapor is considered in the MLS atmosphere at SZA = 30° and albedo = 0.2 (molecular scattering is omitted).

[13] In the 1000–14,280 cm<sup>-1</sup> IR spectral region a method described in part 1 has been applied to create k-distribution channels in each band. Subsequently, the above-discussed technique has been used to get representative cross sections. It was found that if channel absorption is strong or moderately strong, the representative cross sections are not much dependent on atmospheric conditions (pressure and temperature). Figure 3 illustrates this statement. It shows the water vapor representative cross sections

in the most absorbing channel of the 4400–8200 cm<sup>-1</sup> region, which have been obtained for tropical (SZA = 30°) and subarctic winter (SZA = 75°) atmospheres. As one can see the differences between the curves, whose origin the differences in pressure and temperature dependence in the two atmospheres, are really small in comparison with the changes due to W. So in FKDM we used  $\bar{K}(W)$  functions obtained for tropical atmosphere slightly corrected by a scalar factor that depends on the surface temperature  $T_s$  as  $\sim (1/T_s)^G$  (parameter  $G \geq 0$ ). This allowed us to use only 3–4 channels in each band to take into account water vapor absorption whereas in the work of *Chou and Lee* [1996] the use of 7–10 channels was suggested.

[14] For channels with weak absorption, the usual pressure-P- and temperature-T-dependent fit has been used [e.g., *Chou and Suarez*, 2002]:

$$\bar{K}(P, T) = B_1 * (1.0 - B_2 * (300 - T)) * P^B, \quad (3)$$

where  $B_1$ ,  $B_2$  and  $B$  are parameters. In the H<sub>2</sub>O case the self-broadened continuum also has been taken into account as a gray absorber, using the analytical fit borrowed from the CKD model:

$$\bar{K}(P, T)_{\text{self}} = C_1 * 3.2^{(300-T)/C}, \quad (4)$$

where  $C_1$  and  $C$  are the other parameters.

[15] All the fifteen FKDM channels are shown in Table 3, where the first-named gas is the key species. In the troposphere, as it well known, the water vapor absorption dominates in the 1000–14,280 cm<sup>-1</sup> region. So there is only one channel in FKDM where the key species is CO<sub>2</sub>,

**Table 3.** Channel Allocation

| Channel  | Limits, $\text{cm}^{-1}$ ( $\mu\text{m}$ ) | Solar Flux, $\text{W m}^{-2}$ | Rayleigh Scattering Coefficient, $\text{km}^{-1} \text{K atm}^{-1}$ | Species in Channel   |
|----------|--|-------------------------------|---|--|
| 1        | 33,000–50,000 (0.2–0.303)                  | 17.01                         | 63.59   | $\text{O}_3$ , $\text{O}_2$  |
| 2        | 31,000–33,000 (0.303–0.323)                | 13.33                         | 34.48   | $\text{O}_3$   |
| 3        | 14,280–31,000 (0.323–0.7)                  | 607.95                        | 6.406   | $\text{O}_3$ , $\text{H}_2\text{O}$                                |
| 4        | 8200–31,000 (0.323–1.22)                   | 9.45                          | 0.5382  | $\text{O}_2$   |
| 5        | 8200–14,280 (1.22–0.7)                     | 278.86                        | 0.53820   | $\text{H}_2\text{O}$ , $\text{O}_3$ , $\text{O}_2$                 |
| 6        | 8200–14,280 (1.22–0.7)                     | 85.24                         |   | $\text{H}_2\text{O}$ , $\text{O}_3$                                |
| 7        | 8200–14,280 (1.22–0.7)                     | 73.53                         |   | $\text{H}_2\text{O}$   |
| 8        | 1000–8200 (1.22–10.0)                      | 14.16                         | 0.0   | $\text{CO}_2$ , $\text{H}_2\text{O}$                               |
| 9        | 4400–8200 (1.22–2.27)                      | 123.60                        | 0.0598  | $\text{H}_2\text{O}$ , $\text{CO}_2$                               |
| 10       | 4400–8200 (1.22–2.27)                      | 25.66                         |   | $\text{H}_2\text{O}$ , $\text{CO}_2$                               |
| 11       | 4400–8200 (1.22–2.27)                      | 26.16                         |   | $\text{H}_2\text{O}$ , $\text{CO}_2$                               |
| 12       | 4400–8200 (1.22–2.27)                      | 47.04                         |   | $\text{H}_2\text{O}$ , $\text{CO}_2$                               |
| 13       | 1000–4400 (2.27–10.0)                      | 18.96                         | 0.0   | $\text{H}_2\text{O}$ , $\text{CO}_2$                               |
| 14       | 1000–4400 (2.27–10.0)                      | 13.16                         |   | $\text{H}_2\text{O}$ , $\text{CO}_2$                               |
| 15       | 1000–4400 (2.27–10.0)                      | 18.34                         |   | $\text{H}_2\text{O}$ , $\text{CO}_2$                               |
| Total 15 | 1000–50,000 (0.2–10.0)                     | 1372.18                       |   | $\text{H}_2\text{O}$ , $\text{O}_3$ , $\text{O}_2$ , $\text{CO}_2$ |

despite the very strong  $4.3 \mu\text{m}$  absorption band; this is sufficient because of reduced solar radiation in this band. However, in the stratosphere,  $\text{CO}_2$  absorption becomes more noticeable and this gas instead of water vapor should be considered as the key species in some channels. It is the main source of errors in FKDM stratospheric heating rates (errors can reach 2–3% above 70 km). Of course, addition of 1–2 channels in which  $\text{CO}_2$  is the key species can easily decrease these errors, but at the present time it does not appear to be necessary. *Chou and Suarez* [2002] also used one channel for  $\text{CO}_2$ . A detailed FKDM description is provided in Tables 1 and 2.

[16] Here FKDM consists of 15 channels instead of the 38 channels in the work of *Chou and Suarez* [2002], 228 channels in the work of *Kato et al.* [1999], 20 channels

( $\text{CO}_2$  and  $\text{O}_2$  the minor gases only) in the work of *Cusack et al.* [1999], 18 channels ( $\text{CO}_2$  is excluded) in the work of *Nakajima et al.* [2000]. Thus our model has less channels than other models and it has by  $\sim 2.5$  times fewer channels than the model by *Chou and Suarez* [2002] with a similar treatment of gaseous absorption.

[17] Figure 4 shows heating rate errors defined as differences between FLBLM and FKDM calculations for standard atmospheres, such as tropical (TRP), midlatitude summer (MLS), midlatitude winter (MLW), subarctic summer (SAS), subarctic winter (SAW) and “US-standard” (USA), with  $\text{SZA} = 30^\circ$  and surface albedo = 0.2. As can be seen, the errors are  $\sim 0.1 \text{ K d}^{-1}$  below 30 km and  $\sim 0.5 \text{ K d}^{-1}$  above 30 and below 70 km. In addition, Table 4 shows FLBLM and FKDM fluxes for the same conditions. Thus

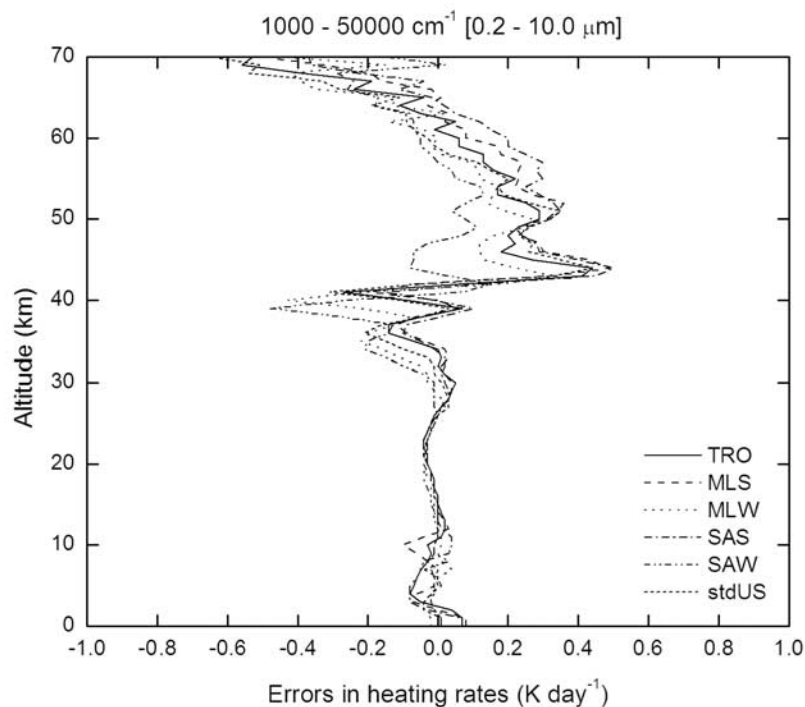


**Figure 4.** Heating rate error profiles for standard tropical (solid line), midlatitude summer (long-dashed line), midlatitude winter (dotted line), subarctic summer (dash-dotted line), subarctic winter (dashed–double-dotted line) and the standard U.S. (short-dashed line) atmospheres ( $\text{SZA} = 30^\circ$ , albedo = 0.2).

**Table 4.** Downward Fluxes at the Surface  $F_{\downarrow}$ , Upward Fluxes at the TOA  $F_{\uparrow}$  and Atmospheric Absorptions AA Calculated by FLBLM and FKDM for the Standard Atmospheres<sup>a</sup>

|                        | SZA = 30° |       |        |       |        |       | SZA = 75° |       |       |       |       |       |
|------------------------|-----------|-------|--------|-------|--------|-------|-----------|-------|-------|-------|-------|-------|
|                        | TRP       | MLS   | MLW    | SAS   | SAW    | USA   | TRP       | MLS   | MLW   | SAS   | SAW   | USA   |
| $F_{\downarrow}$ (LBL) | 946.6     | 963.3 | 1017.8 | 980.7 | 1044   | 998.3 | 252.8     | 257.8 | 277.1 | 263.8 | 287.2 | 270.3 |
| $F_{\downarrow}$ (KD)  | 946.2     | 962.5 | 1018.1 | 979.4 | 1045.2 | 998.2 | 250.5     | 255.9 | 275.6 | 262.2 | 285.7 | 269   |
| $F_{\uparrow}$ (LBL)   | 174.4     | 177.7 | 190.2  | 181.7 | 196.6  | 185.8 | 48.1      | 49.0  | 53.0  | 50.3  | 55.1  | 51.6  |
| $F_{\uparrow}$ (KD)    | 173.0     | 176.4 | 188.5  | 180.2 | 194.8  | 184.3 | 47.2      | 48.4  | 52.5  | 49.7  | 54.6  | 51.2  |
| AA (LBL)               | 256.9     | 240.4 | 184.1  | 222.3 | 156.7  | 204.1 | 104.9     | 100   | 80.6  | 93.9  | 70.3  | 87.3  |
| AA (KD)                | 258.7     | 242.2 | 185.6  | 224.8 | 157.6  | 205.7 | 107.6     | 102.1 | 82.2  | 95.7  | 72.1  | 88.9  |

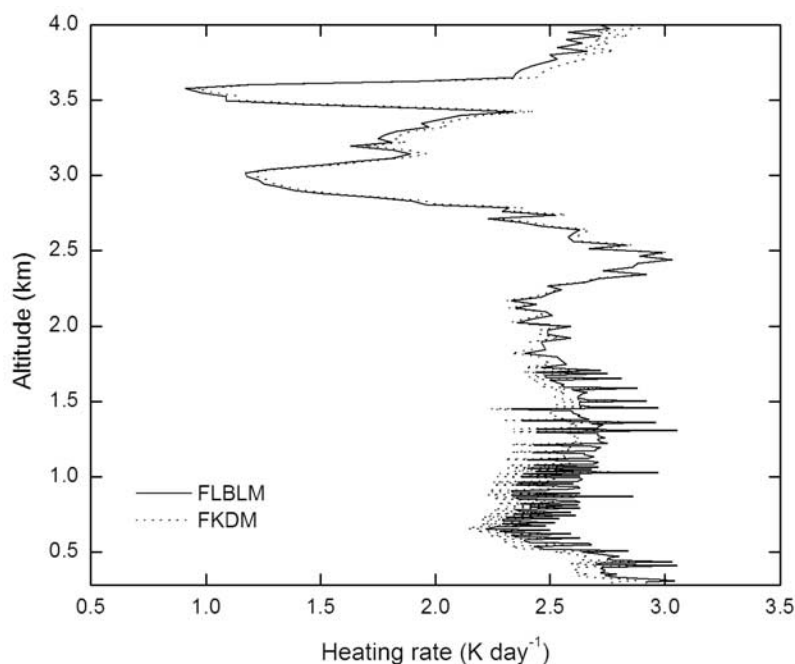
<sup>a</sup> $F_{\downarrow}$ ,  $F_{\uparrow}$ , and AA are given in  $\text{W m}^{-2}$ . LBL, FLBLM; KD, FKDM. Surface albedo = 0.2. Molecular scattering is neglected.

downward flux errors are below 1%, upward flux errors are below 2% (usually  $\sim 1.5 \text{ W m}^{-2}$ ) and total atmospheric absorption errors are below 3% (usually  $1.5\text{--}3 \text{ W m}^{-2}$ ) in all these cases.

[18] To continue our validation, we have also used a case of an observed tropical atmosphere (Amazon region, September 2002) and four cases of observed atmospheres from the SPECTRE campaign. The temperature and humidity profiles in these cases have been taken directly from balloon borne soundings. The profiles have rather complex structure and vertical resolution of 10–100 m in contrast to smooth standard profiles with vertical resolution of 1 km. It is important for validation that these profiles differ both in the water vapor column ranging from 0.55 to 3.57 cm and in surface temperature varying from 272.8 K to 298.5 (see details in part 1). Figure 5 shows FLBLM and FKDM heating rates for the observed tropical atmospheric case with albedo = 0.2 and SZA = 30°. The discrepancies are seen to be below  $0.2 \text{ K d}^{-1}$  even for these complex heating rates. In this case FLBLM/FKDM downward fluxes at the surface, upward fluxes at the TOA and total atmospheric absorption

are  $965.0/963.4$ ,  $179.3/177.7$  and  $237.3/240.2 \text{ W/m}^2$ , respectively. Very similar errors were obtained for the SPECTRE profiles.

[19] We also performed a set of calculations with the same atmospheric models adding molecular scattering. Both FLBLM and FKDM treated scattering by means of the same Monte-Carlo program. As expected, the molecular scattering slightly changed the FKDM accuracy despite it noticeably changed upward and downward fluxes and slightly changed total atmospheric absorption and heating rates. For example, in MLS atmosphere with SZA = 30° and albedo = 0.2 we obtained by FLBLM and FKDM, respectively,  $921.8$  and  $919.5 \text{ W m}^{-2}$  for the downward fluxes at the surface,  $209.1$  and  $208.1 \text{ W m}^{-2}$  for the upward fluxes at the TOA and  $241.9$  and  $244.8 \text{ W m}^{-2}$  for the atmospheric absorptions. Thus differences between these and the corresponding calculations from Table 4 (second column) are  $\sim 40 \text{ W m}^{-2}$  in the downward fluxes at the surface,  $\sim 30 \text{ W m}^{-2}$  in the upward fluxes at the TOA and  $\sim 2 \text{ W m}^{-2}$  in the atmospheric absorptions. Whereas errors in calculations with and without scattering are as follows: 0.25% and 0.08% for the

**Figure 5.** FLBLM (solid line) and FKDM (dotted line) heating rates for the balloon-borne temperature and humidity sounding in the tropical atmosphere.

**Table 5.** FLBLM and FKDM Fluxes Absorbed Inside the Cloud<sup>a</sup>

|                      | 1.8–2.0 km |        |        | 12.8–13.0 km |        |        |
|----------------------|------------|--------|--------|--------------|--------|--------|
|                      | FLBL       | FKDM-1 | FKDM-2 | FLBL         | FKDM-1 | FKDM-2 |
| F, W m <sup>-2</sup> | 80.3       | 96.3   | 89.2   | 129.0        | 142.6  | 140.6  |
| Error, %             | –          | 20     | 11     | –            | 11     | 9      |

<sup>a</sup>Fluxes are given in W m<sup>-2</sup>. ICRCM cases 49 and 47 are used (LWP = 200 g/m<sup>2</sup>, optical thickness  $\tau_{0.55} \sim 9.7$ , MLS atmosphere, surface albedo = 0.2, and SZA = 30°).

downward flux, 0.5% and 0.7% for the upward flux and 1.2% and 0.8% for the atmospheric absorption. Changes in the heating rate errors were found negligible (less than  $\sim 0.01$  K d<sup>-1</sup>).

### 3. Particulate Absorption and Scattering

[20] All k-distribution codes use effective single-scattering properties of clouds and aerosols, which are the same for all the channels of the given band. The fastest of these codes [e.g., *Cusack et al.*, 1999; *Briegleb*, 1992] used in climate models included only three IR bands (0.69–1.19), (1.19–2.38) and (2.38–10.0)  $\mu\text{m}$ , as suggested by *Slingo* [1989]. Here we follow parameterization suggested by *Chou and Suarez* [2002] where similar set of bands is used. Unfortunately the absorption coefficient  $\sigma_A$  and, consequently, the single-scattering co-albedo of cloudy media,  $1 - \omega$ , strongly depend on wave number and vary by several orders of magnitude within these bands. Averaging is therefore necessary and there are several approaches to derive this averaging. In the most recent codes [e.g., *Fu*,

1996; *Chou and Suarez*, 2002] a mix of linear and logarithmic averaging depending on the strength of band absorption is used. However, it should be stressed [*Chou and Suarez*, 2002, p. 14] “that no optimal method has been found for deriving  $\omega$  over a broad band” and so a problem of this deriving will be considered in our paper.

[21] To illustrate this problem, we performed some numerical experiments using so-called “CL” cloud suggested by the Intercomparison of Radiation Codes in Climate Models (ICRCM) working group [*Fouquart et al.*, 1991]. This cloud (LWP = 200 g/m<sup>2</sup>, optical thickness  $\tau_{0.55} \sim 9.7$  at the wavelength  $\lambda = 0.55$   $\mu\text{m}$ ) was inserted in the midlatitude summer atmosphere (surface albedo = 0.2) between 1.8–2.0 km (the ICRCM case 49) and 12.8–13.0 km (the ICRCM case 47). Table 5 presents the FLBLM and FKDM fluxes (W m<sup>-2</sup>) absorbed inside the cloud (difference between the net fluxes at the cloud boundaries) calculated at SZA = 30°. The column FKDM-1 denotes calculations where linear averaging has been used for the absorption coefficient. The cloud absorption is essentially overestimated in both cases by 20% and 11% for low and high clouds, respectively. The relative error is therefore strongly dependent on cloud height.

[22] *Fu* [1996] demonstrated similar results for the cirrus clouds using *Slingo*’s 24 bands. He also showed that the usage of an empirical mixing of linear and logarithmic averaging can decrease discrepancies by  $\sim 1.5$ –2 fold. However, in this and other works, the reason of these discrepancies has not been explained. However, our technique provides an easy explanation. Figure 6a shows wave

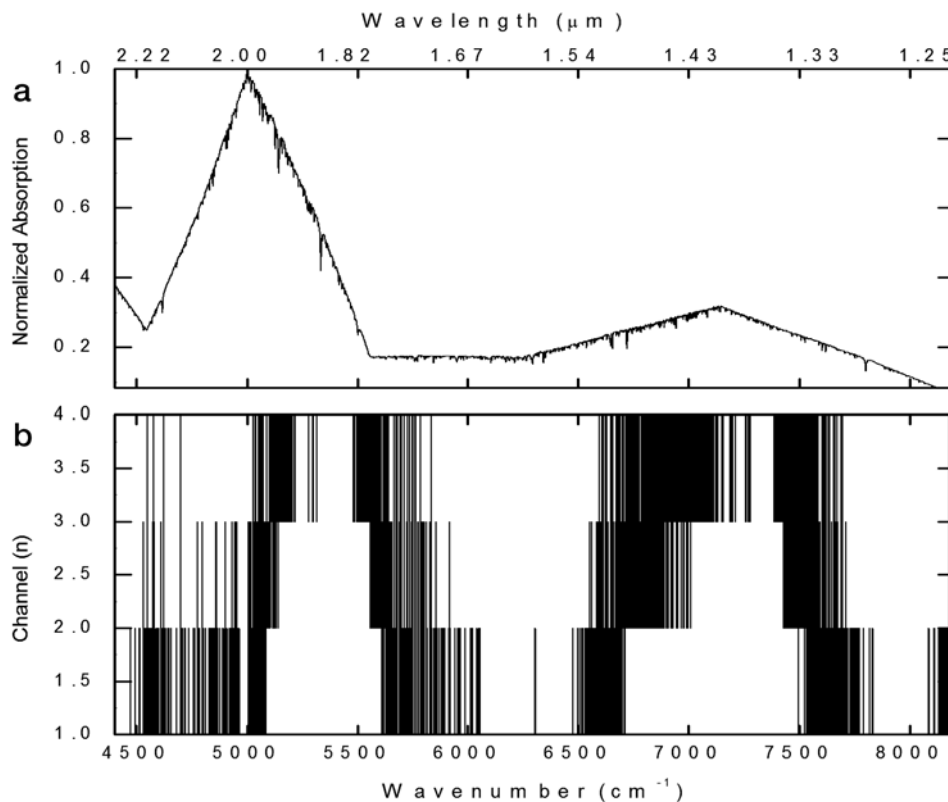


**Figure 6.** Wave number dependence of (a) cloud absorption coefficient multiplied by solar spectrum and (b) wave number channel distribution in the 4400–8200  $\text{cm}^{-1}$  spectral band.

number dependence of the cloud absorption coefficient (multiplied by solar spectrum) calculated using values of complex refractive index from *Hale and Querry* [1973]. Figure 6b shows the wave number channel distribution in the 4400–8200  $\text{cm}^{-1}$  spectral band. Here wave number grid (X-axis) has been obtained by FLBLM with the spectral resolution of  $1/256 \text{ cm}^{-1}$ . Y-coordinate means the channel number (see part 1 for details). The channel's numbers (1, 2, 3 and 4 in our example) are arranged in ascending order of absorption and the weakest absorption of the water vapor is in the first channel, stronger absorption is in the second, etc. Thus the water vapor absorption is the strongest at the wave number points whose Y-coordinate equals 4. As can be seen, these points are concentrated in that spectral region where the cloud absorption (Figure 6a) has maximum. On the other hand the points with the weakest water vapor absorption (Y-coordinate equals 1) are concentrated where the cloud absorption has minimum. Thus both plots show a clear correlation between absorption by cloud drops and channel number, which is caused by the well-known correlation between absorptions in liquid and gaseous water. A small shift between peaks on Figures 6a and 6b is related to the low spectral resolutions in Hale and Querry's table and, consequently, in calculated absorption coefficients as confirmed by using more recent data on the complex refractive index [*Kou et al.*, 1993]. A similar effect exists in the ice clouds also due to the similar correlation between the ice and water vapor absorptions (behavior of refractive indices of water and ice are quite similar; *Kou et al.* [1993]). Consequently, the water vapor above the cloud absorbs solar radiation just in the spectral regions where the cloud absorption is strong. In other words, strong water vapor absorption masks strong cloud absorption. So the effective absorption, which should be obtained using the solar spectrum at the cloud, is less than the above average absorption obtained using the extraterrestrial solar spectrum. Obviously, this effect depends on the water vapor amount above the cloud. It explains why in our numerical experiment the relative errors for low cloud (strong water vapor absorption above the cloud) is essentially greater than the errors for high cloud (weak absorption). It is also clear that a mix of linear and logarithmic averaging or other similar procedure can improve accuracy only under certain atmospheric conditions (e.g., for low clouds in humid atmosphere) but it can cause significant errors in other conditions (for high clouds or clouds in dry atmosphere in our example). The worst of it is that these errors are hardly evaluated, because they depend on varying atmospheric conditions.

[23] Our technique allows the possibility of taking into account the above correlation between absorptions in liquid and gaseous water using average single-scattering properties obtained for each channel separately. To obtain these properties for the given channel, it is necessary to use only the corresponding wave number points (see Figure 6b) in the averaging procedure (e.g., for the fourth channels, only the X-points where the Y-coordinate equals 4 should be used). In the case considered, we obtained the mean channel absorption coefficients  $\sigma_A = 0.288, 0.343, 0.380$  and  $0.435 \text{ km}^{-1}$  for the first, second, third and fourth channels, respectively, whereas the mean band absorption coefficient  $\sigma_A = 0.356 \text{ km}^{-1}$ . Thus in our example the cloud absorption

in channels changes up to  $\sim 1.5$  fold and is rather different from the band mean value. It is easy to understand that these different coefficients define rather different exponential decays of solar radiation in each channel within cloud media and none unit effective absorption coefficient, obtaining by some averaging procedure, can describe fluxes and heating rates in detail.

[24] These channel absorption coefficients and the corresponding coefficients obtained in other bands have been used in our calculations, which is denoted by FKDM-2 in Table 5. As it can be seen taken into account individual absorption coefficients in each channel halves the maximal error so that in both calculations errors now are practically independent on atmospheric conditions and approximately equal to 10%. We have also investigated how usage of mean phase function in each channel improves accuracy but the results showed that it is not very essential (on  $\sim 1\%$  in fluxes absorbed by cloud). Moreover, it was found that usage of single cloud absorption coefficient distorts the simulated heating rates inside the cloud, but this question is beyond the scope of this work. So, in our opinion, the classical k-distribution technique is not effective and needs to be replaced by another one, where each channel should be considered separately and not combined in bands. However, it should be stressed that in contrast to the usual spectral band division (for instance, *Slingo* [1989]) we suggest use of our technique applied to the whole shortwave region, or to wide spectral bands defined by surface reflectance properties.

[25] We performed also some calculations using the same approximate cloud optical properties in FLBLM and FKDM in order to investigate errors outside cloud related to approximate treatment of the gas absorption in FKDM. It was found that these errors are similar to the errors investigated in section 2, which have already been discussed.

#### 4. Summary

[26] A new k-distribution technique for fast shortwave radiation codes has been presented, and an assessment of its accuracy and speed has shown it to be a more efficient technique. In k-distribution terms, characterized by strong absorption, representative absorption cross section is treated as a function of absorber amount along the direct solar radiation path, thus allowing improved fitting of solar fluxes and heating rates in upper troposphere and stratosphere. Moreover, the method allows deriving effective single-scattering properties of clouds separately in each term. It provides more accurate treatment of cloud optical properties by taking into account correlation between water vapor and liquid water or ice absorption. It has been shown that neglect the above correlation in radiation model can distort simulated fluxes and heating rates.

[27] FKDM, which has been developed by means of this technique, has less k-distribution terms than other published models and so offers the best compromise between speed of execution and accuracy in treatment of gaseous absorption in radiation blocks of Global Circulation Models (GCM). In this version of FKDM we used spectral bands division same that used in the widely distributed radiation block by *Chou and Suarez* [2002]. It allows its numerous users to calculate

~2.5 times faster after replacement Chou and Suarez's parameterization by FKDM.

[28] Thus FKDM can be useful right now in increasing of calculation speed. Moreover, it allows to increase an accuracy of calculations in the stratosphere by does not increase the accuracy in the cloudy atmosphere, where we found the principal defect in the existed parameterizations. It is anticipated that future developments in treatment of cloud optical properties separately for each k-term will improve results. This work needs additional efforts, especially in the creating of a set of optical models of clouds and aerosols with high spectral resolution. So it is planned for the next version of FKDM.

[29] **Acknowledgments.** The authors are grateful to Luiz Augusto Toledo Machado and Juan Ceballos for their support and to Tatiana Tarasova for fruitful discussions. The authors also wish to thank Admir Creso Targino for his help. This work has been supported by the CNPq foundation (grant 301263019), Brazil.

## References

- Briegleb, B. P. (1992), Delta-Eddington approximation for solar radiation in the NCAR community climate model, *J. Geophys. Res.*, *97*, 7603–7612.
- Chou, M.-D., and K.-T. Lee (1996), Parameterization for the absorption of solar radiation by water vapor and ozone, *J. Atmos. Sci.*, *53*, 1203–1208.
- Chou, M.-D., and M. J. Suarez (2002), A solar radiation parameterization for atmospheric studies, *NASA/TM-1999-10460, Tech. Rep. Ser. Global Model. Data Assimilation*, vol. 15, 42 pp., NASA Goddard Space Flight Cent., Greenbelt, Md.
- Cusack, S., J. M. Edwards, and J. M. Crowther (1999), Investigating k distributing method for parametrizing gaseous absorption in the Hadley Centre Climate Model, *J. Geophys. Res.*, *104*, 2051–2057.
- Fomin, B. A. (1994), Effective interpolation technique for line-by-line calculations of radiation absorption in gases, *J. Quant. Spectrosc. Radiat. Transfer*, *53*, 663–669.
- Fomin, B. A. (2004), A k-distribution technique for radiative transfer simulation in inhomogeneous atmosphere: 1. FKDM, fast k-distribution model for the longwave, *J. Geophys. Res.*, *109*, D02110, doi:10.1029/2003JD003802.
- Fomin, B. A., and I. P. Mazin (1998), Model for an investigation of radiative transfer in cloudy atmosphere, *Atmos. Res.*, *47-48*, 127–153.
- Fomin, B. A., T. A. Udalova, and E. A. Zhitnitskii (2004), Evolution of spectroscopic information over the last decade and its effect on line-by-line calculations for validation of radiation codes for climate models, *J. Quant. Spectrosc. Radiat. Transfer*, *86*, 73–85.
- Fouquart, Y., B. Bonnel, and V. Ramaswamy (1991), Intercomparing shortwave radiation codes for climate studies, *J. Geophys. Res.*, *96*, 8955–8968.
- Fu, Q. (1996), An accurate parameterization of the solar radiative properties of cirrus clouds for climate models, *J. Clim.*, *9*, 2058–2082.
- Goody, R. M., and Y. L. Yung (1989), *Atmospheric Radiation: Theoretical Basis*, Oxford Univ. Press, New York.
- Hale, G. M., and M. R. Querry (1973), Optical constants of water in the 200  $\mu\text{m}$  to 200 nm wavelength region, *Appl. Opt.*, *12*, 555–563.
- Halthore, R. N., et al. (2005), Intercomparison of shortwave radiative transfer codes and measurements, *J. Geophys. Res.*, doi:10.1029/2004JD005293, in press.
- Kato, S., T. P. Ackerman, J. H. Mather, and E. E. Clothiaux (1999), The k-distribution method and correlated-k approximation for a shortwave radiative transfer model, *J. Quant. Spectrosc. Radiat. Transfer*, *62*, 109–121.
- Kou, L., D. Labrie, and P. Chylek (1993), Refractive indices of water and ice in the 0.65 to 2.5 micron range, *Appl. Opt.*, *32*, 3531–3540.
- Mlawer, E. J., S. A. Clough, P. D. Brown, and D. C. Tobin (1999), Recent development in the water vapor continuum, paper presented at Ninth ARM Science Team Meeting, Atmos. Radiat. Meas. Program, San Antonio, Tex., 22–26 March.
- Nakajima, T., M. Tsukamoto, Y. Tsushima, A. Numaguti, and T. Kimura (2000), Modeling of the radiation process in an atmospheric general circulation model, *Appl. Opt.*, *39*, 4869–4878.
- Ptashnik, I. V., and K. P. Shine (2003), Calculation of solar radiative fluxes in the atmosphere: The effect of updates in spectroscopic data, *Atmos. Oceanic Opt.*, *16*, 251–255.
- Rothman, L. S., et al. (2003), The HITRAN molecular spectroscopic database: Edition of 2000 including updates through 2001, *J. Quant. Spectrosc. Radiat. Transfer*, *82*, 5–44.
- Slingo, A. (1989), A GSM parameterization for the shortwave radiative properties of water clouds, *J. Atmos. Sci.*, *46*, 1419–1427.
- M. de P. Correa and B. Fomin, CPTEC/INPE, Rod. Presidente Dutra, km 40, P. O. Box 01, Cachoeira Paulista, São Paulo 12630-0000, Brazil. (fomin@cptec.inpe.br)